

Chaotic Behaviour in a Three Element Memristor Based Circuit using Fourth Order Polynomial and PWL Nonlinearity

M.H. McCullough and H.H.C. Iu

School of Electrical, Electronic & Computer Engineering
The University of Western Australia
35 Stirling Highway, Crawley, WA 6009, Australia

B. Muthuswamy

Dept. of Electrical Engineering & Computer Science
Milwaukee School of Engineering
Milwaukee, WI 53202

Abstract- This work presents a comparative study of two new chaotic systems obtained from a LCM (inductor-capacitor-memristor) chaotic circuit. We use a fourth order polynomial and piecewise linear nonlinearities for the memristance functions. These systems have only one equilibrium point and use only three fundamental circuit elements, nevertheless, they still generate 2-scroll and 4-scroll attractors. Chaotic behavior is illustrated using phase portraits, bifurcation diagrams and Lyapunov exponent spectra, revealing several chaotic attractors and notably similar dynamical behavior in both systems.

I. INTRODUCTION

The successful fabrication of a memristor in the form of a passive semiconductor device by HP Labs in 2008 [1] has resulted in a significant increase in research into memristors [2] and memristive systems [3]. There currently exists a large body of work examining chaotic behaviour in memristor based circuits, the vast majority of which pertains to systems based on modified Chua's circuits. In 2010, a simpler memristor based circuit comprising of only three elements – a linear passive inductor, a linear passive capacitor and a non-linear active memristor – was shown to be capable of generating a chaotic attractor [4].

This paper presents a comparative study of chaotic behaviour in two new systems based on this three element memristor circuit. The first system is characterized by a continuous fourth order polynomial memristance function. We construct a four segment piecewise-linear approximation of this polynomial function [5] and use it to define the memristance function of the second system. The objective of this study is to confirm the existence of chaos and identify the degree of similarity between the dynamical behaviour in these two systems. These two systems have only one equilibrium point but they still generate multi-scroll attractors. Hence these circuits are more in spirit of general jerk circuits [6] that have a single equilibrium than systems such as Chua's circuit that can generate multiscroll attractors but have multiple equilibrium points [7].

In this work, we present evidence of chaos by way of phase portraits, bifurcation diagrams and Lyapunov exponent spectrums. Our results demonstrate that both systems exhibit similar dynamical behaviour over a range of a given control parameter. This finding will be of potential interest in future studies aimed at constructing physical implementations of memristor emulators capable of generating more complex chaotic behaviour.

II. DYNAMICAL EQUATIONS

The autonomous, three element memristor based circuit presented in [4] consists of a linear passive inductor, linear passive capacitor and a non-linear active memristor in series as shown in Figure 1.

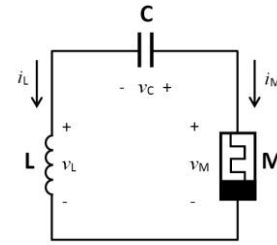


Figure 1 Three element memristor based circuit [4].

We define the state variables for the circuit as

$$x(t) = \begin{pmatrix} v_C(t) \\ i_L(t) \\ z(t) \end{pmatrix}, \quad (1)$$

where $v_C(t)$ denotes the voltage across the terminals of capacitor C , $i_L(t)$ denotes the current flowing through inductor L , and $z(t)$ denotes the internal state variable of the memristor. The first state equation represents the current-voltage relation of the capacitor

$$C \frac{dv_C(t)}{dt} = i_L(t). \quad (2)$$

By applying Kirchhoff's voltage law around the loop we obtain the second state equation

$$L \frac{di_L(t)}{dt} = -(v_C(t) + R(z(t))i_L(t)) \quad (3)$$

where $R(z(t))$ is the memristance function of M .

We define the internal state of the memristor, the final state equation, to be

$$\frac{dz(t)}{dt} = -i_L - \alpha z + i_L^2 z. \quad (4)$$

We chose this particular form of the internal state function based on the state function from [4]. Correspondingly, we also chose the memristance functions (described shortly) as generalizations of the memristance function from [4]. The memristance in [4] had only one minima, our memristance function has two minima and one maxima. The intuitive justification for this choice is

increased complexity of the attractor. Using (2) – (4) we can write the set of state equations for the circuit as

$$\begin{cases} \frac{dv_C(t)}{dt} = \frac{i_L(t)}{C} \\ \frac{di_L(t)}{dt} = -\frac{1}{L}(v_C(t) + R(z(t))i_L(t)) \\ \frac{dz(t)}{dt} = -i_L - \alpha z + i_L^2 z \end{cases} \quad (5)$$

Two systems, System 1 and System 2, are defined based on (5) via the selection of new memristance functions. The memristance functions for each system, R_1 and R_2 respectively, are shown in Figure 2. Memristance function R_1 is a fourth order polynomial defined as

$$R_1(z(t)) = 0.5z(t)^4 - 1.5z(t)^2 - \beta_1. \quad (6)$$

Memristance function R_2 is a four segment piecewise-linear approximation of R_1 defined as

$$R_2(z(t)) = \begin{cases} \delta_a |z(t)| - (\beta_2 + \sigma), & \text{for } |z(t)| > \gamma \\ \delta_b |z(t)| - \beta_2, & \text{for } |z(t)| \leq \gamma \end{cases}, \quad (7)$$

where δ_a , δ_b , γ and σ are selected such that $R_1 = R_2$ at the turning points and roots of each function, for some value of the common control parameter β . In this study the memristance functions have been matched for $\beta_1 = \beta_2 = 1.5$. It should be noted that System 2 will become a less accurate approximation of System 1 as β deviates from the value at which the two functions were matched.

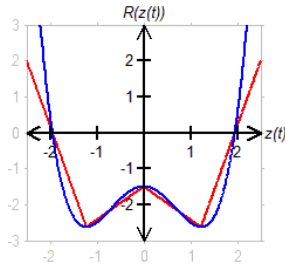


Figure 2 Memristance functions R_1 (blue) and R_2 (red) for the parameters listed in Table 1 and Table 2 with $\beta=1.5$.

III. LINEAR STABILITY ANALYSIS

By setting the left hand side of (5) to zero we can calculate the equilibrium points of the system. By inspection

$$P_0 = ({}^0v_C, {}^0i_L, {}^0z) = (0,0,0) \quad (8)$$

is an equilibrium set for this system. For both systems, it can be shown that the Jacobian at the equilibrium point is given by

$$J(P_0) = \begin{bmatrix} 0 & \frac{1}{C} & 0 \\ -\frac{1}{L} & \frac{\beta}{L} & 0 \\ 0 & -1 & -\alpha \end{bmatrix}. \quad (9)$$

The characteristic polynomial of equation (9) is

$$\lambda^3 + \lambda^2(\alpha - \frac{\beta}{L}) + \lambda(\frac{1}{CL} - \frac{\alpha\beta}{L}) + \frac{\alpha}{CL} = 0, \quad (10)$$

which has roots at

$$\begin{cases} \lambda_1 = -\alpha \\ \lambda_2 = \frac{\beta + \sqrt{-(4L - \beta^2 C)/C}}{2L} \\ \lambda_3 = \frac{\beta - \sqrt{-(4L - \beta^2 C)/C}}{2L} \end{cases}. \quad (11)$$

From (11) it can be seen that there will always be at least one unstable root for $\beta > 0$, thereby yielding the possibility of chaotic behaviour.

Table 1 Simulation Parameters for System 1.

Simulation parameters	Values
Inductance L	3H
Capacitance C	1F
α	0.9
β_1	Control parameter

Table 2 Simulation Parameters for System 2.

Simulation parameters	Values
Inductance L	3H
Capacitance C	1F
α	0.9
β_2	Control parameter
σ	5.5751
γ	1.2247
δ_a	3.6336
δ_b	-0.9186

III. SIMULATION RESULTS

System 1 and System 2 have been simulated using the parameters presented in Table 1 and Table 2 respectively. By setting control parameter $\beta_1 = 2$ for System 1 and $\beta_2 = 1.25$ for System 2 we generate the phase portraits shown in Figures 3a and 3b respectively. Both trajectories form two-lobe chaotic attractors of similar shape and dimensions. Increasing the control parameters such that $\beta_1 = 2.4$ and $\beta_2 = 1.39$ yields similar stable limit cycles in each system, as shown in Figures 4a and 4b. Setting $\beta_1 = 3$ and $\beta_2 = 2$ results in the generation of four-lobe chaotic attractors as shown in Figures 5a and 5b.

By sampling values of $v_C(t)$ where $i_L(t) = z(t) = 0$ for $0 \leq \{\beta_1, \beta_2\} \leq 4$ we generate the bifurcation diagrams, as shown in Figures 6a and 6b. These diagrams show similar dynamical behaviour and bifurcation patterns in both systems. For System 1 (System 2) the first densely populated chaotic region in Figure 6a (6b) corresponds to the two lobe attractor which spans $0 \leq \beta_1 \leq 2.15$ ($0 \leq \beta_2 \leq 1.35$). This is followed by a window of periodic behaviour characterized by the limit cycle shown in Figure 4a (Figure 4b). The second densely populated region of Figure 6a (6b) corresponds to the four lobe attractor and spans $2.55 \leq \beta_1 \leq 3.35$ ($1.44 \leq \beta_2 \leq 2.38$). A third chaotic region can

be seen following a second window of periodic behaviour, however no significant change was observed in the trajectory of the attractor corresponding to this region as compared with Figures 5a and 5b.

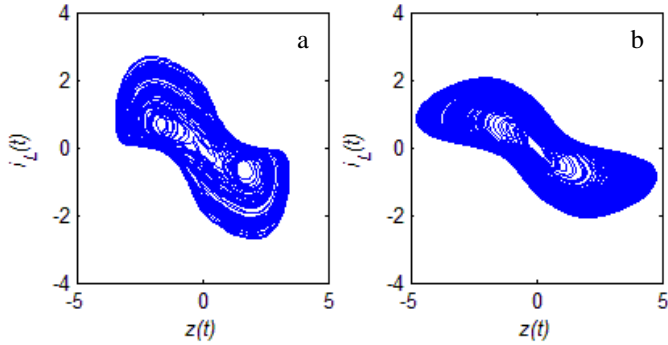


Figure 3 Phase portraits for System 1 $\beta_1=2$ (Figure 3a) and System 2 $\beta_2=1.25$ (Figure 3b).

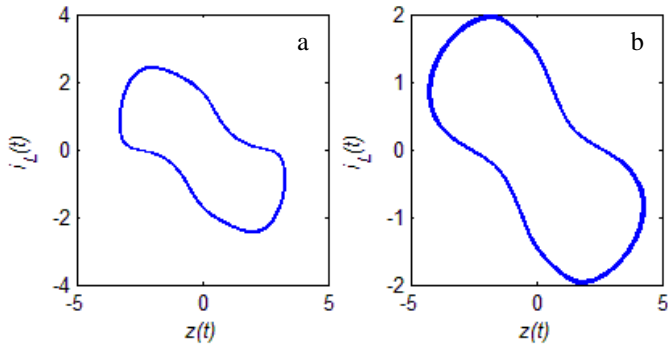


Figure 4 Phase portraits for System 1 $\beta_1=2.4$ (Figure 4a) and System 2 $\beta_2=1.39$ (Figure 4b).

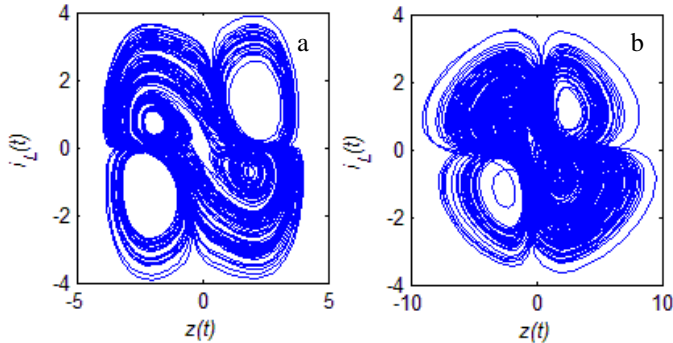


Figure 5 Phase portraits for System 1 $\beta_1=3$ (Figure 5a) and System 2 $\beta_2=2$ (Figure 5b).

Figures 7a and 7b show bifurcation diagrams for control parameter α from equation (4) over the range $0 \leq \alpha \leq 2$ where $\beta_1 = \beta_2 = 1.5$. These figures show multiple chaotic regions and discontinuities. As α decreases over the approximate range $2 \geq \alpha \geq 1$ in Figure 7a, we can see a reoccurring pattern whereby the system, starting as a stable limit cycle, transitions through a period doubling route to chaos followed by another bifurcation into another stable limit cycle (or sometimes chaos) with a smaller trajectory. A similar bifurcation pattern, albeit more discontinuous, can be observed for $2 \geq \alpha \geq 1$ in Figure 7b. Dense chaotic regions interspersed with short windows of periodic behaviour are present in both Figures 7a and 7b for the approximate range $0.3 \leq \alpha \leq 1$.

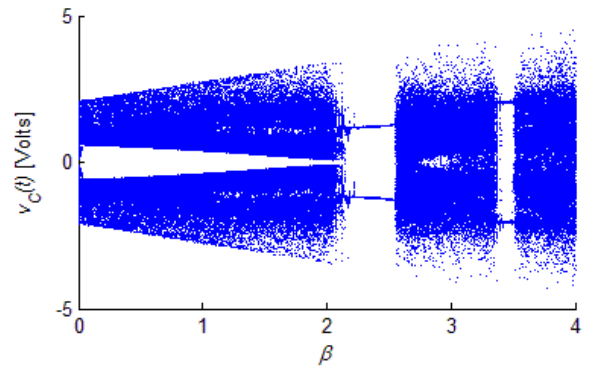


Figure 6a Bifurcation diagram of System 1 for $v_c(t)$ against β_1 .

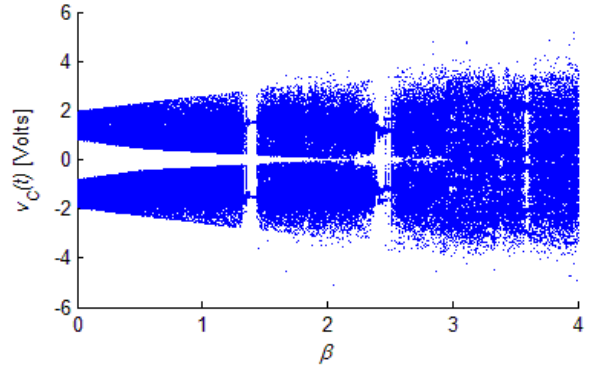


Figure 6b Bifurcation diagram of System 2 for $v_c(t)$ against β_2 .

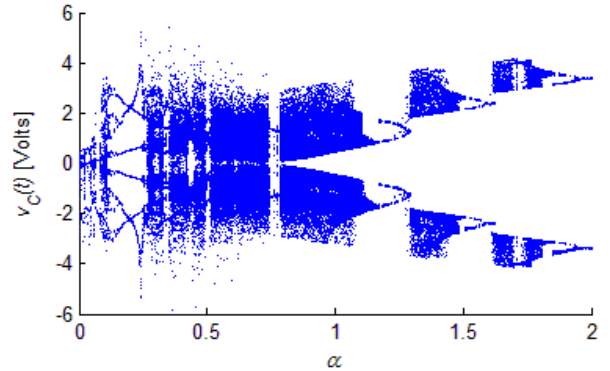


Figure 7a Bifurcation diagram of System 1 for $v_c(t)$ against α .

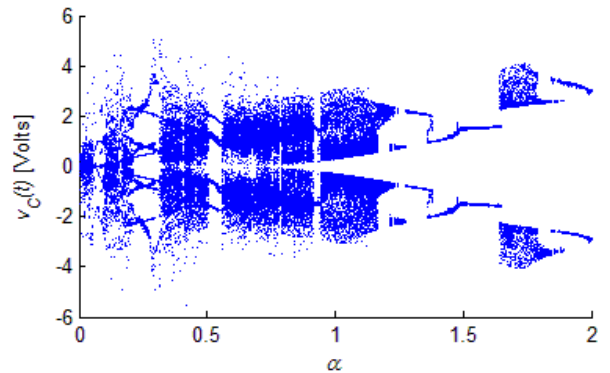


Figure 7b Bifurcation diagram of System 2 for $v_c(t)$ against α .

The spectrum of Lyapunov exponents can provide empirical evidence of chaos [8]. For the three dimensional system in (5) we have exponents $\lambda_1, \lambda_2, \lambda_3$ where $\lambda_1 > \lambda_2 > \lambda_3$. If a system produces a stable limit cycle, the resulting Lyapunov spectrum will meet the conditions

$$\lambda_1 = 0 \text{ and } \lambda_2, \lambda_3 < 0, \quad (12)$$

whereas a chaotic system will result in

$$\lambda_1 > 0, \lambda_2 = 0, \text{ and } \lambda_3 < 0. \quad (13)$$

We calculate the Lyapunov exponents numerically using both the time series method [9] and the QR method [10]. Results corresponding to the phase portraits of Figures 3-5 are listed in Table 3. Due to numerical error in the calculation process we can consider $\lambda_i < 0.01$ to be equivalent to $\lambda_i = 0$. As expected, the systems simulated for Figures 3a, 3b, 5a and 5b meet condition (13) thereby empirically confirming chaos, while Figures 4a and 4b meet condition (12).

Figures 8a and 8b are plots of $\lambda_1, \lambda_2, \lambda_3$ for Systems 1 and 2 respectively over the range $0 \leq \{\beta_1, \beta_2\} \leq 4$. The results illustrate the transition between stable and chaotic behaviour arising from variations in the control variable. Furthermore, the regions corresponding to chaos and stability in these figures align well with those of the bifurcation diagrams shown in Figures 6a and 6b.

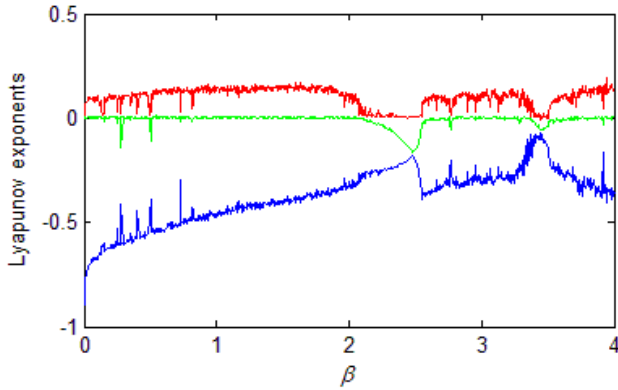


Figure 8a Lyapunov exponent spectrum for System 1 against β_1 .

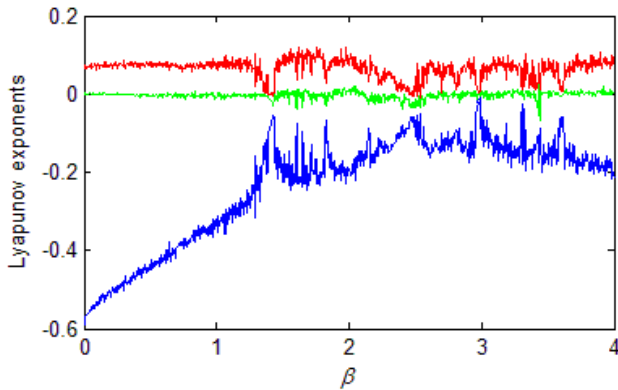


Figure 8b Lyapunov exponent spectrum for System 2 against β_2 .

Table 3 Lyapunov Exponents.

Figure	Simulation parameter	Lyapunov exponents = $\{\lambda_1, \lambda_2, \lambda_3\}$	
		Time Series	QR
3a	$\beta_1 = 2$	{0.076, 0.003, -0.306}	{0.112, 0.000, -0.334}
3b	$\beta_2 = 1.25$	{0.086, -0.003, -0.288}	{0.068, 0.001, -0.264}
4a	$\beta_1 = 2.4$	{0.005, -0.105, -0.219}	{0.001, -0.106, -0.215}
4b	$\beta_2 = 1.39$	{0.002, -0.011, -0.100}	{0.004, -0.011, -0.101}
5a	$\beta_1 = 3$	{0.106, 0.003, -0.312}	{0.098, -0.004, -0.300}
5b	$\beta_2 = 2$	{0.089, 0.008, -0.197}	{0.088, 0.002, -0.188}

V. CONCLUSION

In this paper, we have studied and compared chaotic behaviour in two new systems built from a three element, autonomous memristor based circuit. The existence of several chaotic attractors and stable limit cycles within each system has been demonstrated by way of phase portraits and bifurcation diagrams. Empirical evidence of chaos has been presented in the form of Lyapunov exponent spectrums.

The results have shown that the first system, characterized by a continuous fourth order polynomial memristance function, exhibits similar chaotic behaviour to the second system, whose memristance function is a piecewise-linear approximation of the former. This constitutes a significant finding in that it should be possible to physically implement memristor emulator circuits capable of generating complex chaotic behaviour without the need for resource intensive FPGAs or microcontrollers to model high order non-linearity. Memristor emulators characterized by piecewise-linear non-linearity could potentially be designed and constructed using standard discrete elements.

Currently, we are working on physically emulating the memristor. It would also be interesting to check if n-scroll attractors can be generated from this circuit by an appropriate choice of internal state and memristance functions.

REFERENCES

- [1] D.B. Strukov, G.S. Snider, G.R. Stewart and R.S. Williams, "The missing memristor found," *Nature*, vol. 453, pp. 80-83, Mar. 2008.
- [2] L. O. Chua, "Memristor - The missing circuit element," *IEEE Transactions on Circuit Theory*, vol. 18, pp. 507-519, 1971.
- [3] L.O. Chua and S.M. Kang, "Memristive devices and systems," *Proceedings of the IEEE*, vol. 64, pp. 209-223, 1976.
- [4] B. Muthuswamy and L. O. Chua, "Simplest chaotic circuit," *Int. Journal of Bifurcation and Chaos*, vol. 20, pp. 1567-1580, 2010.
- [5] M. Bucolo, L. Fortuna, M. Frasca and M.G. Xibilia, "A generalized Chua cell for realizing any continuous n-segment piecewise-linear function," *Int. Journal of Bifurcation and Chaos*, vol. 11, no. 9, pp. 2517-2527, 2001.
- [6] S. Yu, J. Lü, H. Leung and G. Chen, "Design and implementation of n-scroll chaotic attractors from a general jerk circuit". *IEEE Transactions on Circuits and Systems I: Regular Papers*, vol. 52, no. 7, pp. 1459 - 1476, 2005.
- [7] T. Matsumoto, L. O. Chua and M. Komuro, "The double scroll," *IEEE Transactions on Circuits and Systems*, vol. 32, no. 8, pp. 797-818, 1985.
- [8] A. Wolf, J. Swift, H. Swinney and J. Vastano, "Determining Lyapunov exponents from a time series," *Physica D: Nonlinear Phenomena*, vol. 16, pp. 285-317, 1985.
- [9] V. Govorukhin, "Calculation Lyapunov exponents for ODE," <http://www.mathworks.com/matlabcentral/fileexchange/4628>, 2004.
- [10] S. Siu, "Lyapunov exponent toolbox," <http://www.mathworks.com/matlabcentral/fileexchange/233>, 1998.